ICARUS 11, 36–45 (1969)

Martian Temperatures and Thermal Properties

DAVID MORRISON, CARL SAGAN, AND JAMES B. POLLACK

Laboratory for Planetary Studies, Center for Radiophysics and Space Research, Cornell University, Ithaca, New York 14850

Communicated by W. M. Sinton

Received February 19, 1969; revised April 11, 1969

We have utilized previously unreduced 8–13 μm radiometry of Mars performed in 1954 by Sinton and Strong to obtain the distribution of temperature over the Martian surface. The temperatures are consistent with predictions obtained from solution of the one-dimensional equation of heat conduction with a thermal inertia of about 0.005 cal cm^{-2} sec$^{-1/2}$ deg^{-1}. This value is also suggested by the mean microwave brightness temperature of about 200°K. At the Martian atmospheric pressure, this inertia would result from average particle sizes of about 100 μm. The thermal inertia of the darkest areas is larger than that of the bright areas, as would be expected if the atmospheric pressure is higher or the mean particle size is larger in the dark areas. The observed latitudinal temperature gradient appears to be consistent with temperatures of approximately 145°K at 60° winter latitudes and therefore with a polar cap composed, at least in part, of CO_2. At all latitudes the minimum temperature falls below 190°K; under these circumstances, a significant fraction of the atmospheric water vapor will condense at night, contributing to the "dawn haze." An analysis of the microwave spectrum of Mars suggests that the loss tangent of the subsurface material is less than 0.03.

I. Introduction

The best data available on the distribution of surface temperatures on Mars are contained in the infrared scans of the disk made by Sinton and Strong during the favorable opposition of 1954 (1960*a*; see also Sinton and Strong, 1960*b*). These authors measured the flux in the 8–13 μm range with a resolution of 1.5 arcsec and a dynamic range in the corresponding temperature running from the maximum near 300°K down to about 180°K.

Of their 33 scans, Sinton and Strong reduced and published the temperature as a function of position for only 6 equatorial scans (1960*a*). In this paper, we discuss the results of a reduction of a total of 31 scans yielding more than 500 independent temperature measurements on the illuminated hemisphere of Mars. From these brightness temperatures, we derive thermometric temperatures and compare them with the predictions of thermal models for the planet.

II. Surface Temperatures

The uncalibrated thermal scans of Mars are given in analog form in a contract report by Sinton and Strong (1960*c*). The reduction of these data to temperatures depends on the brightness temperature of 290°K found for the center of the disk by Sinton and Strong (1960*a*); we show below that this is an otherwise plausible value. We have derived brightness temperatures from the instrumental deflections, using a calculated relationship between blackbody temperature and the amount of blackbody flux that penetrates the atmosphere in the 8–14 μm window; this curve (Morrison, 1968) is similar to that given by Sinton and Strong (1960*b*, Fig. 2) and reproduces their data reduction, at least for temperatures in excess of 220°K. Scans that crossed the

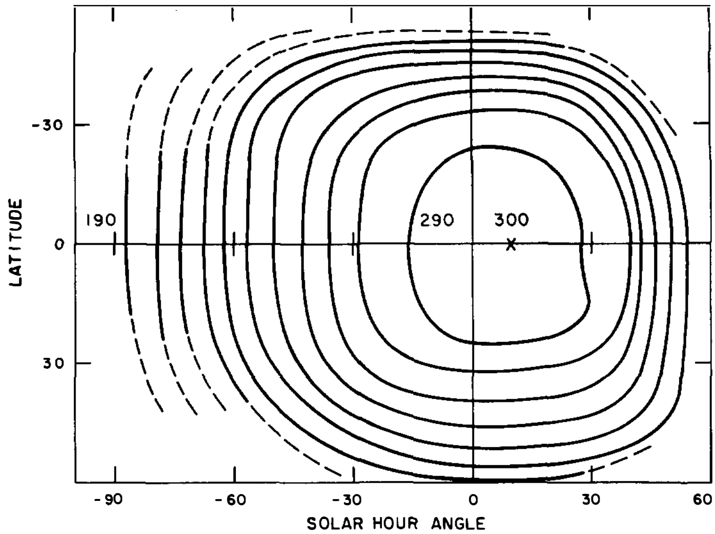

FIG. 1. Brightness temperature map of Mars. All data from bright areas are included. The dashed isotherms are known with less accuracy than the solid lines. Contour interval is 10°.

center of the disk were normalized, the effective aperture being allowed for, to give a temperature of 290°K there, and these scans in turn provided the normalization for the scans that did not cross the center. The deflections were converted to temperatures at intervals of 1 arcsec along each scan, and for each temperature we computed the areographic latitude, longitude, and solar hour angle. We have estimated the systematic errors in the temperatures that may be introduced by the finite areal resolution of the radiometer and by seeing motion of the planet, both of which will result in an overestimate of the temperature near the limb. The errors due to resolution are less than 1%, but seeing motion of a few arcseconds during the 4-sec integration time of the system could increase this to as much as 5%. A complete listing of the reduced data is given by Morrison (1968), where reduction techniques and error analysis are also discussed in more detail.

Scans that cross the prominent dark areas Meridiani Sinus and Margaritifer Sinus near the center of the disk show a temperature 4° to 6° higher in these areas than in the surrounding bright areas. There may also be a small increase for points in Syrtis Major. The effective aperture of 1.5 arcsec was small enough so that the dark areas were not contaminated by adjacent bright areas. When the data for these dark areas are excluded, we obtain the brightness-temperature map for July 1954 given in Fig. 1.

The laboratory measurements made by Hovis and Callahan (1966) on selected powdered terrestrial minerals indicate that the radiometric emissivity of such materials is about 0.93, while the emissivity in the 8–13 μm band is near 0.95, both independent of chemical composition and of temperature (to within less than 2%) in the range 200–300°K. We have converted the brightness temperatures to thermometric temperatures by dividing by the nth root of 0.95, where we take the 8–13 μm flux to be proportional to temperature to the nth power, so that n is given by $1.44/\lambda T$ when λT is in cm-deg. This approximation is valid provided $n \gtrsim 3$, as it is for these wavelengths and Martian temperatures. We have also made the conversion on the assumption that the Martian emissivity has a mean value of 0.95 but shows a variation with direction like that found by Sinton (1962) for the Moon. Table I gives the equatorial brightness temperatures (T_B) and the two values of the thermometric temperature (T_1 and

TABLE I

EQUATORIAL BRIGHTNESS TEMPERATURES AND THERMOMETRIC TEMPERATURES

Solar hour angle	T_B (°K)	T_1 (°K)	T_2 (°K)	σ_T (°K)	N
−84°	195°	196°	202°	16°	8
−74°	209°	210°	215°	11°	8
−65°	223°	225°	229°	9°	7
−55°	246°	248°	249°	9°	11
−45°	253°	255°	255°	8°	9
−35°	271°	274°	274°	7°	7
−25°	281°	284°	283°	7°	11
−15°	291°	294°	293°	4°	12
−4°	296°	300°	299°	3°	10
+5°	300°	303°	303°	1°	9
+15°	299°	302°	303°	1°	8
+24°	293°	296°	298°	1°	6
+34°	285°	288°	293°	6°	6
+43°	269°	272°	280°	8°	7

T_2) obtained by the above means; it also gives the number of points used in forming each average (N) and the standard deviation of these points about the average (σ_T).

III. COMPARISON WITH THERMAL MODELS

In order to compare with these data, we have computed theoretical surface temperatures for Mars by numerical solution of the plane-parallel, homogeneous one-dimensional partial differential equation for subsurface heat conduction. Since Gierasch and Goody (1968) have shown that the atmosphere of Mars has little effect on the surface temperature, we have not included the atmosphere in these calculations. We have, however, used a constant greenhouse flux of back-radiation to the surface of magnitude 1% of the peak insolation (Gierasch, private communication). For insolation conditions at the time of observation, we find the peak surface temperature as a function of radiometric Bond albedo and of thermal inertia $(K\rho c)^{1/2}$ cal cm^{-2} sec$^{-1/2}$ deg^{-1}, as shown in Fig. 2. The peak temperature given in Table I is 303°K. For the bright areas, we use a radiometric Bond albedo of 0.25, based on the studies of de Vaucouleurs (1964), Tull (1966), Walker (1966), Irvine, Simon, Menzel, Pikoos, and Young (1968), and McCord and Adams (1969). The resulting thermal inertia is between 0.004 and 0.005 cal cm^{-2} sec$^{-1/2}$ deg^{-1}. From the high-resolution differential colorimetry of McCord and Adams (1969) we find that Syrtis Major has a radiometric albedo 0.58 ± 0.10 times that of the predominant bright areas. Applying this ratio to the dark areas studied here, we obtain an albedo of 0.15. With this albedo and a peak temperature of 308°K, the dark area thermal inertia is about 0.006 cal cm^{-2} sec$^{-1/2}$ deg^{-1}. In order for the bright and dark areas to have the same thermal inertia, their peak temperatures would have to differ by 10° for this choice of albedos; alternatively, the thermal inertias could be the same for a 5° temperature difference if the albedos were 0.25 and 0.20, respectively.

Figure 3 compares the equatorial temperatures with those predicted by the heat-conduction calculations for an albedo of 0.25 and two choices of thermal inertia. Both temperatures T_1 and T_2 of Table I are plotted. As indicated above, a thermal inertia of 0.004 cal cm^{-2} sec$^{-1/2}$ deg^{-1} fits very well near the peak; the fit is also acceptable over the rest of the curve, although the 0.006 thermal-inertia curve fits equally well at most hour angles. On the whole, the fit of these two computed curves to the data seems satisfactory, and the values for the thermal inertia of 0.010 suggested by Sinton and Strong (1960*a*) and of 0.002 suggested by Leovy (1966*a*) can probably be excluded. Our values are in agreement, however, with the conclusions of Sinton (1961).

We have computed the expected distribution of temperature on Mars at the equinox (heliocentric longitude of 268°) for the combinations of thermal inertia and bolometric albedo suggested above for the bright and dark areas, with the results shown in Fig. 4. The dark area is always hotter than the bright, although during midmorning this difference is very small. The greatest temperature differences, about 15°, develop in late afternoon and persist throughout the night. If such

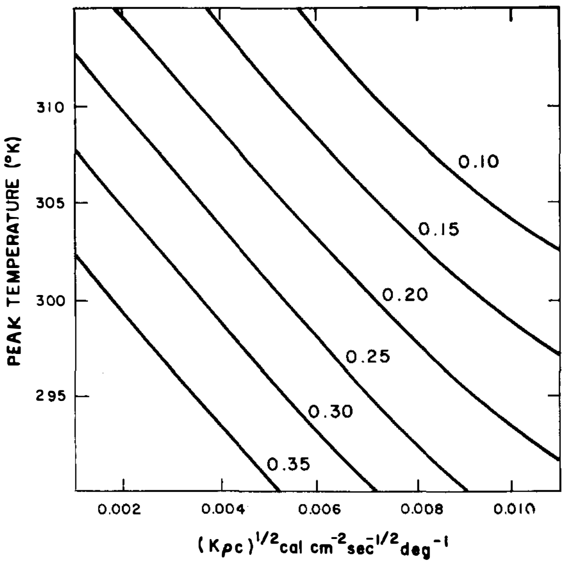

FIG. 2. Peak thermometric surface temperature on Mars as a function of thermal inertia $(K\rho c)^{1/2}$ for a number of radiometric albedos. Computations are made for latitude $-8°$ and heliocentric longitude 290°. The radiometric emissivity was taken to be 0.93.

temperature differences do exist on Mars between adjacent bright and dark areas, they may drive winds analogous to the terrestrial sea breeze.

Using data from north–south scans only, we have found the average variation of brightness temperature with latitude in the bright areas in the three regions of solar

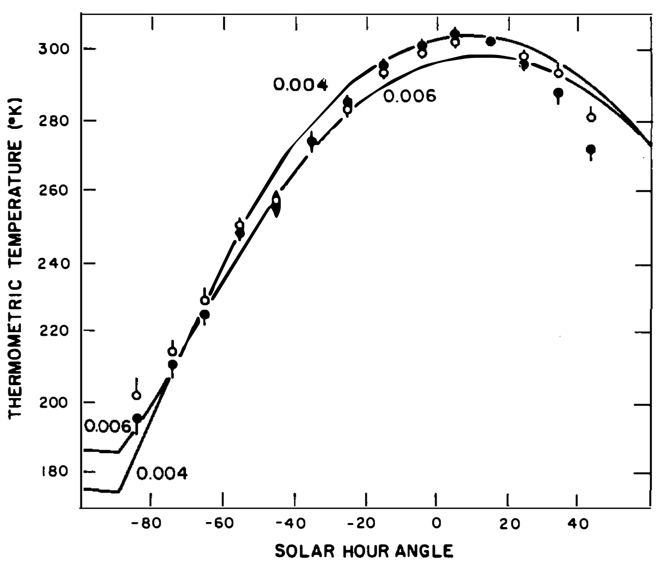

FIG. 3. Comparison of the data with theoretical curves obtained from heat-conduction models. Filled circles are T_1, and open circles are T_2 (see Table I). Only half of each error bar (representing the standard deviation in the mean) is shown. The theoretical curves are labeled by the assumed thermal inertia $(K\rho c)^{1/2}$ cal cm^{-2} sec$^{-1/2}$ deg^{-1}.

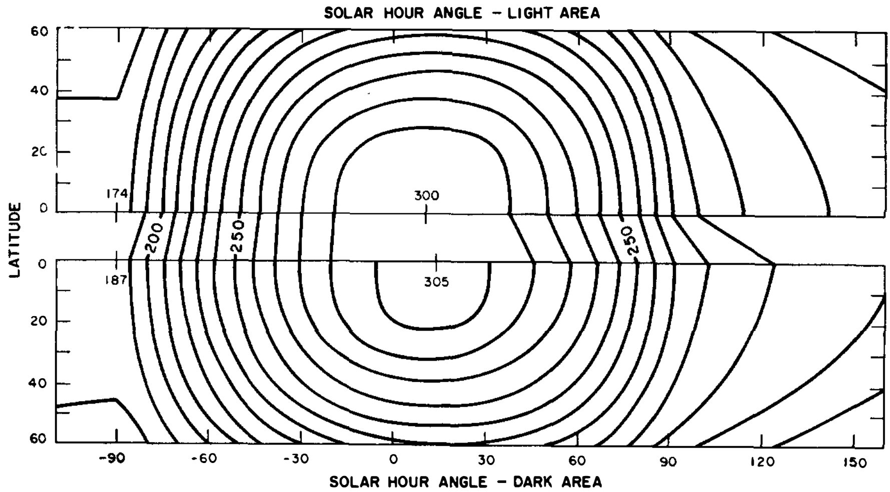

FIG. 4. Theoretical temperature distribution with latitude and solar hour angle for Mars at the equinox (heliocentric longitude, 268°). The upper map was computed for bright areas: albedo, 0.25 and thermal inertia, 0.004 cal cm^{-2} sec$^{-1/2}$ deg^{-1}. The lower map represents dark areas: albedo, 0.15 and thermal inertia, 0.006 cal cm^{-2} sec$^{-1/2}$ deg^{-1}.

hour angle shown in Fig. 5. The curve in this figure is the thermometric temperature expected from the model with thermal inertia 0.004 and bolometric albedo 0.25 at heliocentric longitude 290°. When allowance is made for the difference between brightness temperature and thermometric temperature, the data fit the curve very well in the northern hemisphere. In the south, however, the data show a more rapid temperature drop than at the corresponding positive latitudes, while the theoretical curve drops more slowly. This difference may be due to seasonal effects, which were not allowed for in computing theoretical curves; it was spring in the

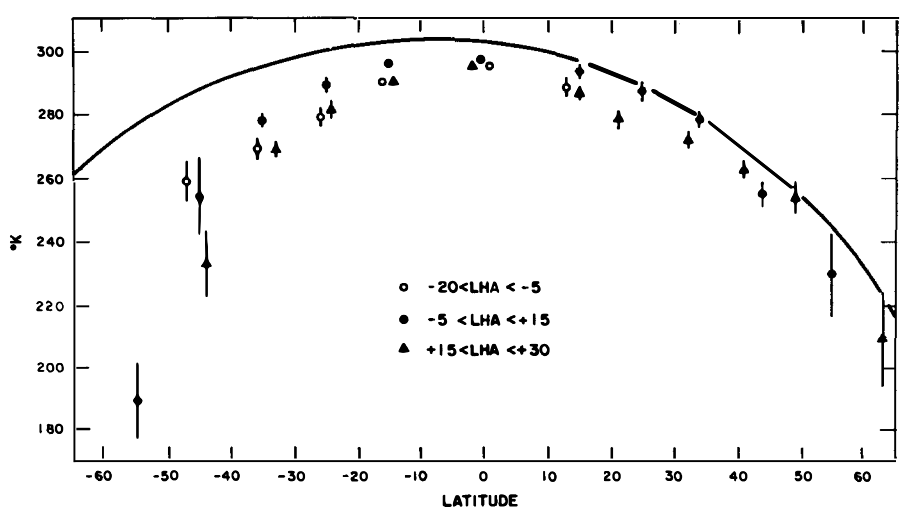

FIG. 5. Variation of temperature with latitude. The data points are average brightness temperatures with indicated standard deviations in the mean. The solid curve is the theoretical peak thermometric temperature for an albedo of 0.25 and a thermal inertia of 0.004 cal cm^{-2} sec$^{-1/2}$ deg^{-1}. This curve should be above the data points by less than 10°K.

southern hemisphere at the time of the observations and the ground was cooler than would be expected from insolation alone. In addition, there was still a large south polar cap. If the cap shrank in 1954 at the same rate as observed in the past (Slipher, 1962), its edge should have been near latitude −60°. The data of Fig. 5 suggest that the temperatures at this latitude were near 160°K and are compatible with a polar cap composed, at least in part, of frozen carbon dioxide at a temperature of 145°K, as suggested by Leighton and Murray (1966), Leovy (1966*b*), and Gierasch and Goody (1968).

IV. Microwave Temperatures

Observations of microwave brightness temperatures can be used to determine δ, the ratio of electrical to thermal skin depths in the subsurface material of a planet. For the Moon and the inferior planets, this information is derived from the variation of temperature with phase, but the range of phase angles available for Mars (±45°) is inadequate for such a study. However, nearly equivalent information can be derived from dayside brightness temperatures measured at millimeter wavelengths. If it is assumed that the net temperature gradient in the subsurface is negligible, that the microwave emissivity is independent of wavelength, and that the range of surface temperatures is approximately known from infrared measurements, then $\delta(\lambda)$, the ratio of skin depths, can be determined directly from the shape of the microwave spectrum. The dayside temperature $T_B(\lambda)$ is computed from the usual equation for the phase effect (Piddington and Minnet, 1949) of a homogeneous planet, evaluated at maximum temperature:

$$T_B(\lambda) = \bar{T}_B + \beta \Delta T_{IR}(1 + 2\delta + 2\delta^2)^{-1/2}, \tag{1}$$

where $\beta \simeq 0.75$ and ΔT_{IR} is the surface temperature variation. At long wavelengths the brightness temperature is approximately equal to $\bar{T}_B$.

The microwave observations of Mars have been summarized recently by Hobbs, McCullough, and Waak (1968) and by Epstein (1968), who find no departure from a flat thermal spectrum. These authors corrected each observed temperature to mean solar distance on the assumption, first suggested by Dent, Klein, and Aller (1965), that the radio temperatures scale as the reciprocal square root of the solar distance. This scaling law leads to an overestimate of the correction to the observed temperatures. While the daytime maximum surface temperature depends on distance in this manner, the nighttime minimum temperature is practically independent of solar distance. We therefore suggest that the radio brightness temperature at short centimeter wavelengths should scale approximately as the average of the maximum and minimum temperatures. At shorter wavelengths, the dependence on distance should become stronger, while at decimeter wavelengths, where the annual as well as the diurnal temperature variations are damped out, no distance correction is needed.

In Fig. 6 we have plotted the published observations of Mars listed by Hobbs

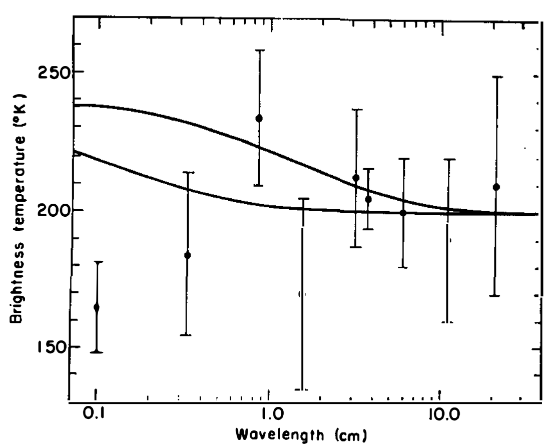

Fig. 6. Microwave observations of Mars. When more than one measurement has been made at a given wavelength, we have plotted the weighted average temperature. The theoretical spectra are computed from Eq. (3); the upper curve is for $\delta/\lambda = 1$ cm^{-1}, the lower curve for $\delta/\lambda = 10$ cm^{-1}. The observed points are normalized to the same flux scale and to mean solar distance.

et al. (1968) and by Epstein (1968). We have applied the modified distance correction discussed above and also, when sufficient information is available, we have adjusted the temperatures to the flux scale of Kellermann, Pauliny-Toth, and Williams (1969; see also Scheuer and Williams, 1968). The largest correction required was a 10% increase in the temperature at 3.75-cm wavelength measured by Dent *et al.* (1965). Also shown in Fig. 6 are the spectra computed from Eq. (1) with $\bar{T}_B = 200°K$ and $\Delta T_{IR} = 55°K$. We assume $\delta(\lambda) \propto \lambda$, as is generally the case for good dielectric materials; the upper curve is for $\delta = \lambda$ and the lower is for $\delta = 10\lambda$ (λ in centimeters). Most of the data appear to be consistent with any value of δ/λ greater than 1 cm^{-1}. However, the 165° temperature at 1-mm wavelength (Low and Davidson, 1965) is not in agreement with any model described by Eq. (1).

The thermal skin depth on Mars is given by

$$L_t = (KP/\pi\rho c)^{1/2} \tag{2}$$

where K is the thermal conductivity, P is the diurnal period in seconds, and ρc is the heat capacity per unit volume. For the particulate material near the surface of Mars, ρc is likely to be about 0.3 cal cm^{-3} deg^{-1}. A thermal inertia of about 0.005 cal cm^{-2} $sec^{-1/2}$ deg^{-1}, as determined from the infrared data, therefore implies $K \cong 8 \times 10^{-5}$ cal cm^{-1} sec^{-1} deg^{-1} and $L_t \cong 3$ cm. The electrical skin depth, L_e, is then greater than 3λ, since the data indicate that $\delta/\lambda > 1$ cm^{-1}.

The electrical skin depth for a dielectric can be related to the more readily observed quantity, the loss tangent ($\tan\Delta$), as follows (see Pollack and Sagan, 1965):

$$L_e = \lambda/2\pi\epsilon^{1/2}\tan\Delta, \tag{3}$$

where ϵ is the dielectric constant ($\cong 3$ for Mars). From this expression we find that the material in the upper few centimeters of the Martian subsurface is characterized by $\tan\Delta < 0.03$. This upper limit excludes many minerals in the solid form, but it is compatible with the presence on Mars of a wide range of minerals in a particulate or powdered state. A value of $\tan\Delta = 0.003$, corresponding to the lower curve in Fig. 6, is comparable to that of the Moon and Mercury.

The mean temperature of $200° \pm 10°K$ derived from the long-wavelength microwave observations can be compared with values predicted from the thermal models, employing different values of the thermal inertia. The brightness temperature is the product of the equilibrium thermometric temperature and the disk-averaged microwave emissivity, $\bar{e}$. The radar reflectivity of Mars at wavelengths of 12.5 cm and 43 cm is about 5% for the bright areas and about 10% for the dark (Dyce, 1965), from which we derive values of $\bar{e}$ of 0.90 and 0.86 for the bright and dark areas, respectively. We have computed the equinoctial equilibrium temperatures to be expected for the choices of albedo and thermal inertia previously derived for the bright and dark areas, averaging over the disk using techniques developed for the planet Mercury (Morrison and Sagan, 1967; Morrison, 1969). When corrected to mean solar distance and multiplied by the emissivity $\bar{e}$ (assumed independent of wavelength), the disk-averaged brightness temperatures for both models are $195° \pm 5°K$, almost independent of the fraction of the disk occupied by bright and dark areas. High-resolution radiometry of Mars should find little temperature difference between light and dark areas at microwave frequencies. The agreement between the predicted and observed disk temperature of Mars should not be overemphasized, since the observations were not made when the rotation axis was perpendicular to the line of sight, as was assumed in the calculations, and since we do not know how seasonal effects might modify the computed temperature. However, the fact that the observed radio temperature is as low as $200° \pm 10°K$ excludes equatorial minimum temperatures as high as 210°K (as has been suggested by Öpik, 1966), irrespective of postulated thermal processes during the Martian night. Within the context of simple heat conduction models, values of the thermal inertia much higher than 0.010 cal cm^{-2} $sec^{-1/2}$ deg^{-1} are incompatible with the radio data.

V. Discussion

The preceding analysis shows that the most probable values for the thermal inertias of the bright and dark areas are 0.0045 ± 0.001 and 0.006 ± 0.001 cal cm^{-2} $sec^{-1/2}$ deg^{-1}, respectively. These values characterize the top few centimeters of the subsurface. For $\rho c = 0.3$ cal cm^{-3} deg^{-1}, the values of the thermal conductivity corresponding to these inertias are $(7 \pm 3) \times 10^{-5}$ and $(12 \pm 4) \times 10^{-5}$ cal cm^{-1} sec^{-1} deg^{-1}.

Leovy (1966*a*) has summarized a number of experimental determinations of the thermal conductivity of mineral powders as a function of atmospheric pressure. At the Martian average pressure of 5–10 mb (Fjeldbo and Eshleman, 1968), these conductivities depend strongly on particle size but only very weakly on chemical composition. For the values of the thermal conductivity quoted above, the mean particle sizes are 25–250 μm and 100–300 μm for the bright and dark areas, respectively. These values, which are larger than those found by Leovy (1966*a*), are in agreement with particle mean sizes of 50 μm and 160–800 μm obtained for the bright and dark areas by Pollack and Sagan (1969) from an analysis of Martian photometry and polarimetry.

Recent radar mapping of Martian topography along latitude +22° (Pettengill, Counselman, Rainville, and Shapiro, 1969) shows elevation differences of up to 12 km between parts of the planet which are, within the definitions of this paper, all bright areas. Since each data point that we used in constructing the temperature profile of the bright areas (Table I) is an average of measurements at a variety of longitudes, it is appropriate to use the mean pressure in the interpretation of these bright area temperatures. However, Binder (1969) suggests from the same radar data that the major dark areas are systematically lower than the bright areas. In this case, the particle sizes derived above will be too large. The difference that we find in thermal conductivity between the bright and dark areas may therefore be due either to differences in mean elevation or to differences in mean particle size or to both if the difference is real.

Spectrographic studies (Kaplan, Münch, and Spinrad, 1964; Schorn, Spinrad, Moore, Smith, and Giver, 1967) indicate that the mean water-vapor content of the Martian atmosphere is about 10^{-3} gm cm^{-2}. Assuming that this water vapor is concentrated in the lower few kilometers of the troposphere, the water-vapor mixing ratio is of order 10^{-4} and the saturation vapor pressure is reached at temperatures near 200°K. The minimum equatorial temperatures indicated in this study are between 170° and 180°K. According to calculations by Gierasch and Goody (1968), convective stirring in the atmosphere is inhibited during the night, but radiative transfer processes will lead to a temperature below 200°K in the lower half-kilometer of the atmosphere. Thus any water vapor present in this portion of the atmosphere will undergo condensation. In addition, horizontal winds may induce vertical motion, leading to an introduction of water vapor from the upper layers of the atmosphere and thus to further condensation (see Sagan, Levinthal, and Lederberg, 1968). Since this condensate will persist an hour or more after sunrise, it may be identified with the "dawn haze." In view of the afternoon temperatures predicted in Fig. 4, it seems unlikely that water vapor could condense at the surface to form the midafternoon clouds reported by many observers (see, e.g., de Vaucouleurs, 1954; Slipher, 1962).

The quantitative results presented here for Martian temperatures and thermal properties are ultimately based upon the accuracy of the absolute temperature calibration for the center of the disk obtained by Sinton and Strong (1960*a*). As shown by Fig. 2, an error of a few degrees in the peak temperature will make a not insignificant difference in the deduced thermal inertia. It is, however, encouraging that the thermal inertia derived from Fig. 2 for a peak temperature of 303°K also generates a theoretical curve that is in good agreement with the data over the entire observed range of solar hour angle, without any *ad hoc* assumptions being required. While the results also depend strongly on the choice of radiometric albedos, these are now known with sufficient accuracy. The emissivities are less certain, but the results are little affected if we choose alternative values. Future thermal observations that include the evening as well as morning quadrants of the planet will be valuable in extending these studies, as will high-resolution radiometry to be done from Mariner space probes.

In conclusion, this analysis of previously unpublished data yields a distribution of temperature on the illuminated hemisphere of Mars that is consistent with a simple theoretical heat-conduction model and with observations of the disk-averaged microwave brightness temperature. We find for the thermal inertia a value larger than that deduced by Leovy (1966*a*) but somewhat smaller than the value originally given by Sinton and Strong (1960*a*) and subsequently used by Leighton and Murray (1966) and Geirasch and Goody (1968). The variation of temperature with latitude seems to be consistent with a polar-cap temperature of 145°K, and even at the equator we note that nighttime temperatures are low enough for atmospheric water vapor to condense.

Note added in proof: A recent laboratory determination of the electromagnetic loss properties at 38 GHz (8mm wavelength) of goethite and limonite, two minerals often suggested as comprising a substantial fraction of the Martian surface material, has kindly been communicated to us by M. J. Campbell. Using these data, we find that a loss tangent of less than 0.03, as suggested in this paper, requires a specific density of less than 3 for goethte and less than 1 for limonite. Densities in this range are compatible with the measured low values of the thermal conductivity and of the radar cross section of the planet.

Acknowledgments

We wish to thank Peter Gierasch, M. J. Klein, Nancy D. Morrison, and William Sinton for helpful discussions. This research was supported in part by NASA Grants NGR 09-015-023 and NGR 33-010-082. One of us (DM) acknowledges the support of a Smithsonian Research Foundation Fellowship.

References

Binder, A. B. (1969). Topography and surface features of Mars. *Icarus,* in press.

Dent, W. A., Klein, M. J., and Aller, H. D. (1965). Measurements of Mars at λ 3.75 cm from February to June, 1965. *Astrophys. J.* **142**, 1685.

Dyce, R. (1965). Recent radar observations of Mars. *Proc. Caltech-JPL Lunar and Planetary Conf., JPL Tech. Mem.* **33-266.**

Epstein, E. E. (1968). Mars, Jupiter, and Saturn: 3.4 mm brightness temperatures. *Astrophys. J.* **151**, 2199.

Fjeldbo, G., and Eshleman, V. R. (1968). The atmosphere of Mars analysed by integral inversion of the Mariner IV occultation data. *Planet. Space Sci.* **16**, 1035.

Gierasch, P., and Goody, R. (1968). A study of the thermal and dynamical structure of the Martian lower atmosphere. *Planet. Space Sci.* **16**, 615.

Hobbs, R. W., McCullough, T. P., and Waak, J. A. (1968). Measurements of Mars at 1.55-cm and 0.95-cm wavelengths. *Icarus* **9**, 360.

Hovis, W. A., and Callahan, W. R. (1966). Infrared reflectance spectra of igneous rocks, tuffs, and red sandstones from 0.5 to 22 μ. *J. Opt. Soc. Am.* **56**, 639.

Irvine, W. M., Simon, T., Menzel, D. H., Pikoos, C., and Young, A. T. (1968). Multicolor photoelectric photometry of the brighter planets. III. Observations from Boyden Observatory. *Astron. J.* **73**, 807.

Kaplan, L. D., Münch, G., and Spinrad, H. (1964). An analysis of the spectrum of Mars. *Astrophys. J.* **139**, 1.

Kellermann, K. I., Pauliny-Toth, I. I. K., and Williams, P. J. S. (1969). The spectra of radio sources in the revised 3C catalogue. *Astrophys. J.*, in press.

Leighton, R. B., and Murray, B. C. (1966). Behavior of carbon dioxide and other volatiles on Mars. *Science* **153**, 136.

Leovy, C. (1966*a*). Note on thermal properties of Mars. *Icarus* **5**, 1.

Leovy, C. (1966*b*). Mars ice caps. *Science* **154**, 1178.

Low, F. J., and Davidson, A. W. (1965). Lunar observations at a wavelength of 1 mm. *Astrophys. J.* **142**, 1278.

McCord, T. B., and Adams, J. B. (1969). Spectral reflectivity of Mars. *Science* **163**, 1058.

Morrison, D. (1968). Martian surface temperatures. *Smithsonian Astrophys. Obs. Spec. Rept.* **284**.

Morrison, D. (1969). Thermal models and microwave temperatures of the planet

Mercury. *Smithsonian Astrophys. Obs. Spec. Rept. No.* **292**.

MORRISON, D., AND SAGAN, C. (1967). The microwave phase effect of Mercury. *Astrophys. J.* **150**, 1105.

ÖPIK, E. J. (1966). The Martian surface. *Science* **153**, 255.

PETTENGILL, G. H., COUNSELMAN, C. C., RAINVILLE, L. P., AND SHAPIRO, I. I. (1969). Radar measurements of Martian topography. *Astron. J.*, **74**, 461.

PIDDINGTON, J. H., AND MINNET, H. C. (1949). Microwave thermal radiation from the Moon. *Australian J. Sci. Res., Series A*, **2**, 63.

POLLACK, J. B., AND SAGAN, C. (1965). The microwave phase effect of Venus. *Icarus* **4**, 62.

POLLACK, J. B., AND SAGAN, C. (1969). An analysis of Martian photometry and polarimetry. *Space Sci. Rev.*, **9**, 243.

SAGAN, C., LEVINTHAL, E., AND LEDERBERG, J. (1968). Contamination of Mars. *Science* **159**, 1191.

SCHEUER, P. A. G., AND WILLIAMS, P. J. S. (1968). Radio spectra. *Ann. Rev. Astron. Astrophys.* **6**, 321.

SCHORN, R. A., SPINRAD, H., MOORE, R. C., SMITH, H. J., AND GIVER, L. P. (1967). High-dispersion spectroscopic observations of Mars. II. The water-vapor variations. *Astrophys. J.* **147**, 743.

SINTON, W. (1961). Recent radiometric studies of the planets and the moon. *In* "Planets and Satellites, The Solar System," (G. P. Kuiper and B. M. Middlehurst, eds.), Vol. III. Univ. of Chicago press, Chicago, Illinois.

SINTON, W. (1962). Temperatures on the lunar surface. *In* "Physics and Astronomy of the Moon" (Z. Kopal, ed.), p. 407. Academic Press, New York.

SINTON, W., AND STRONG, J. (1960*a*). Radiometric observations of Mars. *Astrophys. J.* **131**, 459.

SINTON, W., AND STRONG, J. (1960*b*). Radiometric observations of Venus. *Astrophys. J.* **131**, 470.

SINTON, W., AND STRONG, J. (1960c). Observations of the infrared emission of planets and determination of their temperatures. *ONR Contract Rept. No.* **248(01)**.

SLIPHER, E. C. (1962). "Mars: The Photographic Story" Sky Publ. Corp., Cambridge, Massachusetts.

TULL, R. G. (1966). The reflectivity spectrum of Mars in the near-infrared. *Icarus* **5**, 505.

VAUCOULEURS, G. P., DE (1954). "Physics of the Planet Mars." Faber and Faber, London.

VAUCOULEURS, G. P., DE (1964). Geometric and photometric parameters of the terrestrial planets. *Icarus* **3**, 187.

WALKER, R. (1966). Infrared photometry of stars and planets. Thesis, Harvard University, Cambridge, Massachusetts.